Bond formation in titanium fulleride compounds studied through x-ray emission spectroscopy

Mats Nyberg,[1] Yi Luo,[1] L. Qian,[2] J.-E. Rubensson,[2] C. Såthe,[2] D. Ding,[3] J.-H. Guo,[2] T. Käämbre,[2] and J. Nordgren[2]
[1]*Department of Physics, Stockholm University, P.O. Box 6730, S-113 85 Stockholm, Sweden*
[2]*Department of Physics, Uppsala University, Box 530, S-751 21 Uppsala, Sweden*
[3]*Institute of Atomic and Molecular Physics, State Key Lab for Superhard Materials, Jilin University, Changchun 120023, P. R. China*
(Received 31 May 2000; published 2 March 2001)

The geometric and electronic structures of titanium fulleride complexes have been studied at the gradient corrected density-functional theory level by using various $C_{60}Ti_x$ ($x=1,2$) clusters. The cluster with the Ti atom binding on the six-ring site (η^6) of the fullerene is shown to be lower in energy than those with Ti atom adsorbed on either five-ring (η^5) or bridge (η^2) sites. The bond formation for titanium fulleride has further been examined by calculated nonresonant, resonant, and off-resonant x-ray emission spectra of the clusters, and a comparison to the experimental counterpart. The examination shows that only the theoretical spectra of clusters with a six-ring adsorption site are in close agreement with the experimental x-ray emission spectra of titanium fulleride films. Our results indicate that off-resonant x-ray emission spectra provide an excellent basis for the probing of the bonding between metals and organic molecules.

DOI: 10.1103/PhysRevB.63.115117 PACS number(s): 61.48.+c, 71.15.Mb

I. INTRODUCTION

The unique physical and chemical properties of fullerenes and their derivatives have attracted great attention in the last decade. The reactions of metal atoms with fullerenes resulted in the formation of a set of compounds that possesses some interesting properties, e.g., superconductivity.[1,2] Numerous metal complexes with fullerenes have been synthesized and examined by different experimental techniques. However, due to the complexity of these compounds, it is very difficult to fully understand the electronic and geometrical structures, bond formation, and bond strengths solely from experimental measurements. Theoretical calculations, therefore, are expected to play an important role. Indeed, the theoretical studies based on the first-principle methods have provided valuable insights for different fullerenes and their derivatives, ranging from geometries to spectroscopies and properties.[3,4] The geometrical structures of some endohedral metal fullerides in which a metal atom, generally a nontransition metal atom, is encapsulated within a fullerene, have also been reported.[4]

In the present paper, we will focus on the transition metal fullerides. As the first test case, titanium fulleride compounds have been chosen because of the existence of relatively rich experimental results. From the pattern of the abundant titanium-fullerene clusters in the mass spectrum and the reactivity towards O_2 and CO, it was proposed that titanium is binding to the six-membered ring.[5] The formation of titanium-fulleride was also characterized experimentally by the use of x-ray photoelectron spectroscopy, Raman spectroscopy,[6] x-ray absorption, and x-ray emission spectroscopies.[7] X-ray emission spectroscopy, in particular, can provide information of the valence orbitals, and thus, can also be used in order to understand bond formation of such complexes. However, the size and complexity of the transition metal fullerides makes it almost impossible to analyze the experimental x-ray emission spectra in great detail without the help of theoretical simulations.

The Hartree-Fock (HF) approach has been successfully applied to the x-ray emission of fullerenes.[8] However, due to the lack of correlation effects, it is difficult to apply the HF approach to the metal complexes. From a theoretical point of view, it is of importance to examine the applicability of the density-functional theory to the x-ray emission of metal complexes with fullerenes, since this is the only correlated method that is applicable to such big systems.

II. THEORETICAL DETAILS

All the calculations in this paper have been done at the gradient corrected density-functional theory (DFT) level, using the exchange functional by Perdew and Wang and the correlation functional by Perdew.[9] For this purpose, we have used the density-functional code DEMON,[10] in which three different basis sets are used, namely a normal orbital basis set and two auxiliary basis sets, in order to provide a balanced description for core, valence, and Rydberg orbitals.

In all the calculations, valence double-zeta plus polarization basis sets were used for the carbon atoms, including 3, 2, and 1 contractions for *s*, *p*, and *d*, respectively. For titanium, a double-zeta basis set was used with 5, 4, and 2 contractions for *s*, *p*, and *d*, respectively. The x-ray emission spectra are generated by the group theory formulation developed by Luo *et al.*[8,11] Such a computational procedure has been successfully applied to free molecules,[12] oligomers,[13] fullerenes,[8] and adsorbates.[14] The transition moments between the initial, intermediate, and final states are calculated based on the ground-state wave function. Therefore, intermediate- and final-state relaxation effects are neglected. The effects of intermediate state lifetime broadening and incoming photon distribution have been exclusively considered. We used a value of 0.08 eV for the lifetime of the intermediate state, which is a typical value for the core excited state of carbon and 0.20 eV for the width of the incoming photon distribution.

III. EXPERIMENTAL DETAILS

The experiment was performed at the beamline 7.0 of advanced light source (ALS), Lawrence Berkeley Labora-

tory. This beamline, using the U5 type undulator and an SGM monochromator,[15] provides radiation in soft x-ray region with a high brightness and high-energy resolution. The C K x-ray emission spectra were measured using a high-resolution grazing-incidence soft x-ray spectrometer with a two-dimensional multichannel detector.[16] The emission spectra were taken with the spectrometer resolution set at about 0.6 eV when the grating of 4001/mm and the slit width of 20 μm are used in the experiment. Calibration of the photon energy in the emission spectra was determined by the π^* peak of C_{60} film from x-ray absorption spectra, which was measured in the total fluorescence yield. The $Ti_{1.7}C_{60}$ sample was made by coevaporation of C_{60} and metallic Ti from a Knudsen-type effusion cell and an *e*-beam evaporator, respectively, in an ultrahigh vacuum deposition chamber. A Si(100) substrate was chosen and situated approximately 10 cm away from the sources. The processes of the film preparation and characterization have been described in detail in Refs. 6 and 7. Since the prepared film is degraded in air due to oxidation, a capping layer (500 Å titanium) on the sample surface deposited to protect the sample transferred to an experimental station in ALS.

IV. GEOMETRY OPTIMIZATIONS AND TOTAL ENERGY CALCULATIONS

From patterns of abundant transition metal-C_{60} clusters in mass spectra and reactivity towards O_2, CO, NH_3, C_2H_4, and C_6H_6, it has been concluded that transition metals can be bonded either with hexagon rings, pentagon rings, or bridged between two carbon atoms of C_{60} depending on the transition metal involved. For instance, it seems that early transition metals, e.g., Sc, Ti, and V, are preferentially ligated with six-membered rings (η^6) of C_{60}, while late transition metals, e.g., Fe, Co, and Ni often sit either atop (η^3) or on a bridge (η^2) site of C_{60}.[17,18,5] Very recently, small Ni_m $(C_{60})_n$ clusters have been studied using the tight-binding molecular dynamics method,[19] and the results seem to confirm the experimental observations for the late transition metals. However, until present date, there are no theoretical studies for the early transition-metal-C_{60} clusters. The η^6 ligand found for the early transition metals is quite special, since it was known that, in general, for the transition metal complexes with C_{60}, the C_{60} acts as an η^2 ligand.[2]

We have optimized the geometry of Ti adsorbed on C_{60} for three different bonding sites, namely the η^2, the η^5, and the η^6 sites, using $C_{60}Ti_1$ and $C_{60}Ti_2$ clusters, see Fig. 1.

The resulting geometrical values are presented in Table I below, together with the binding energy of the Ti atoms. Inspection of this table shows that the Ti atom binds in an unsymmetric fashion when we try to place it in the five-ring, exhibiting a very short bond distance (1.92–1.94 Å), two medium-short bond distances (2.09 Å) and two long bond distances (2.37–2.39 Å). This adsorption site is therefore more properly described as an ontop or a threefold adsorption site.

The binding energies for bridge and five-ring adsorption are very similar, and significantly smaller than the six-ring value, both for one and two Ti atoms adsorbed. As can also be seen from these results, the binding energy for a Ti atom does not change significantly when we add an extra Ti atom to the system, which means that the effects due to the charging of the C_{60} cage are small. This flexibility is consistent with the fact that C_{60} is a good electron acceptor.

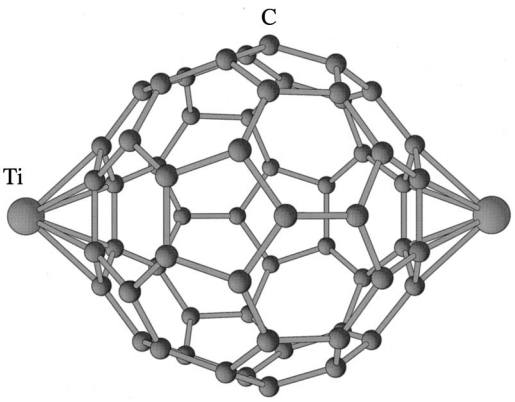

FIG. 1. The optimized structure for $C_{60}Ti_2$.

V. BONDING SCHEME AND RESONANT INELASTIC X-RAY SCATTERING

The bonding between metal atoms and organic molecules has often been described by the so-called Dewar, Chatt, and Duncanson model (DCD), which is based on a frontier orbital concept.[20,21] The interaction has often been viewed as a donation of charge from the highest occupied (π) orbital into the metal and a subsequent back donation from filled metal states into the lowest unoccupied (π) orbital. A schematic picture of the bonding between a Ti atom and C_{60} is shown in Fig. 2. The *d* orbitals of the Ti atom, the highest occupied molecular orbital (HOMO) $4h_u$ and the lowest unoccupied molecular orbital (LUMO) $5t_{1u}$ are energetically favorable to involve into the bonding. Within the donation/back-donation scheme, new orbitals of the d-t_{1u} type should be found in the occupied orbital space, and orbitals with the d-h_u mixture can be expected in the unoccupied space. We will show that such a bonding scheme can be verified by the resonant inelastic x-ray scattering (RIXS).

RIXS spectroscopy is a combination of x-ray absorption

TABLE I. Binding energies (BE) of the Ti atoms (in eV/atom) and bond distances (in Å) of $C_{60}Ti$ and $C_{60}Ti_2$ from the present DFT calculations. The numbers in parenthesis give the number of bonds associated with the bond lengths.

System	BE	Ti-C distance
$C_{60}Ti_1$		
Bridge	3.57	2.03
Five-ring	3.35	1.92(1), 2.09(2), 2.37(2)
Six-ring	4.01	2.16(2), 2.17(4)
$C_{60}Ti_2$		
Bridge	3.43	2.03
Five-ring	3.42	1.94(1), 2.09(2), 2.39(2)
Six-ring	3.78	2.17(2), 2.21(4)

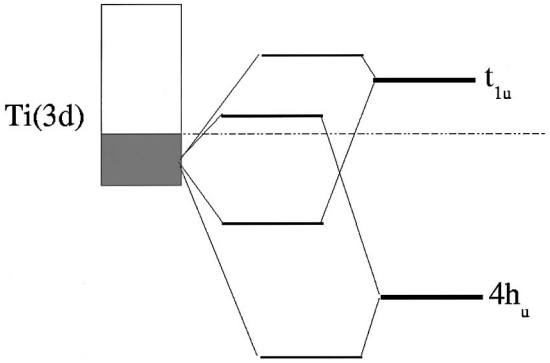

FIG. 2. A simple picture of the bond formation between Ti and C_{60}.

and emission processes, which can simply be represented as

$$A+\hbar\omega \rightarrow A_c^* \rightarrow A_v^* + \hbar\omega',$$

where A_c^* and A_v^* denote the excited core and valence states, respectively. ω and ω' are the frequencies of incoming and scattered photons. In this section we will go through some basic concepts that will help in the interpretation of the RIXS results presented in this paper. For this purpose, a simplified few-level model is used, as shown in Fig. 3. In this diagram, we have for simplicity included only two unoccupied levels (1 and 2, representing the π^* and the hybridized bonding orbitals, respectively), one carbon core-level (0) and one occupied valence level (3).

For a given frequency of an incoming photon, the frequency of an emitted photon should fulfill the energy conservation law,

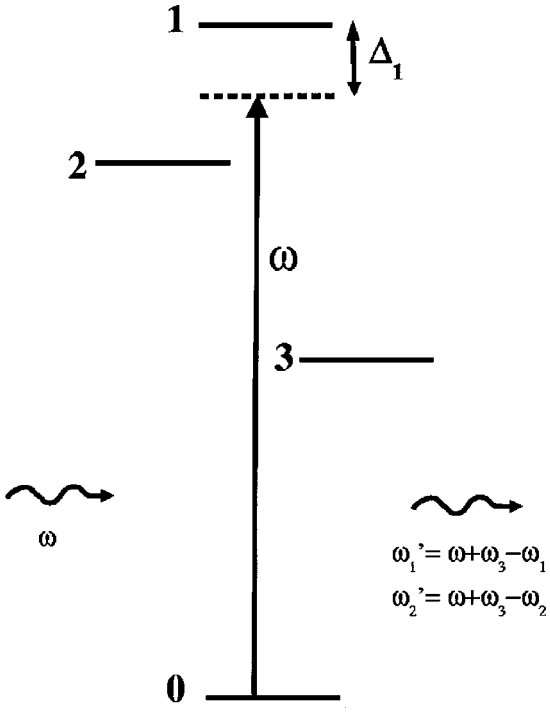

FIG. 3. An illustration of the RIXS spectroscopy of a four-level system.

$$\omega = \omega' + \omega_{\nu n}, \tag{1}$$

where ν and n represent the unoccupied and occupied orbitals, respectively. For our four-level model, the emitted photons should exhibit two different frequencies due to the two different scattering channels, 0-2-3 and 0-1-3. Therefore, we have

$$\omega_1' = \omega+\omega_3-\omega_1 \quad \omega_2' = \omega+\omega_3-\omega_2. \tag{2}$$

The cross sections of two scattering channels can be expressed as

$$\sigma_1(\omega_1') = \frac{\mu_1^2\mu_3^2}{\Delta_1^2+\Gamma^2} \quad \sigma_2(\omega_2') = \frac{\mu_2^2\mu_3^2}{(\Delta_1+\omega_{12})^2+\Gamma^2}, \tag{3}$$

where $\Delta_1 = \omega-\omega_1$, the detuning energy from the π^*, and $\omega_{12} = \omega_1-\omega_2$, the energy difference of the two unoccupied orbitals. In general, the transition moment between the core level and the π^* level (μ_1) is much larger than that between the core level and the hybridized bonding level (μ_2), which has more metal character. Therefore, in principle, one should be able to observe the scattering signal from channel one at any excitation photon frequency. The channel two outgoing photons can be observed when the ratio

$$r_{21} = \frac{\mu_2^2}{\mu_1^2}\frac{\Delta_1^2+\Gamma^2}{\mu_1^2(\Delta_1+\omega_{12})^2+\Gamma^2} \tag{4}$$

is large enough. This condition can be fulfilled when the incoming photon is nearly resonant to the bonding orbital, $\Delta_1+\omega_{12}\approx 0$ or when the hybridization is strong enough to result in a large value for μ_2. We will use the principle outlined above to discuss the x-ray emission spectra of $C_{60}Ti$ complexes.

A. Nonresonant x-ray emission

The experimental nonresonant x-ray emission spectra of C_{60} and $C_{60}Ti_{1.7}$ compounds are shown in Fig. 4. The only visible difference between these two spectra is in the highest energy region, where the two distinguishable peaks for C_{60} are smeared out by the adsorption of the Ti atoms. This can be seen as an indication that the geometric and electronic structure of C_{60} have been slightly modified by the bonding of the Ti atoms.

The theoretical nonresonant x-ray emission spectra of C_{60} and $C_{60}Ti$ at different bonding sites are also illustrated in Fig. 4. The width of the valence band of C_{60} calculated using DFT was found to be compressed when we compared it to the experimental one, which probably is due to the neglect of the relaxation effects. A better agreement between theory and experiment was found after scaling the calculated orbital energies by a factor of 1.3 followed by an energy shift of 288.6 eV. For the calculated spectrum in Fig. 4, and all the presented calculated spectra in this paper, we have employed this scaling procedure. It can be worth mentioning that an opposite effect was found using Hartree-Fock for the calculation of C_{60} RIXS spectra,[8] where instead it was necessary to compress the calculated spectrum with a factor of 1.2. The

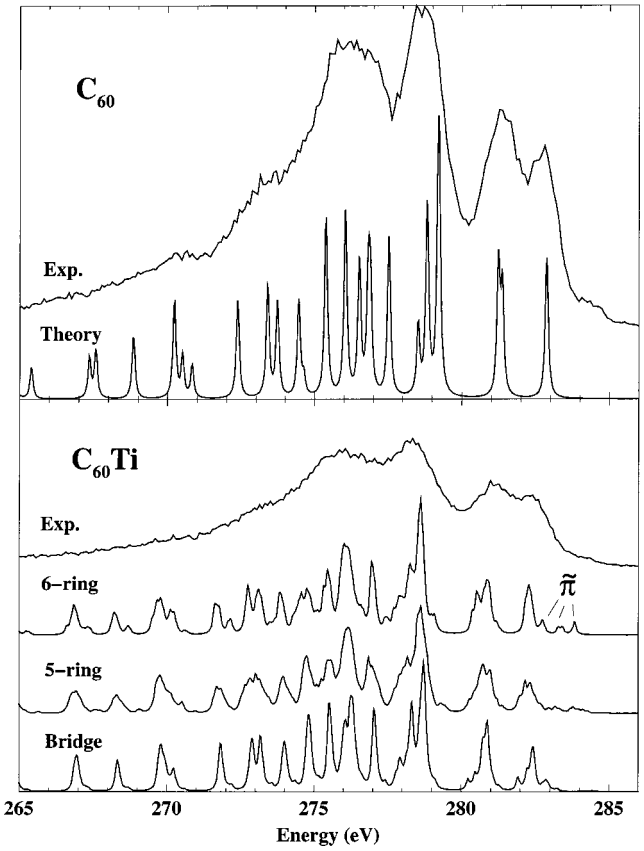

FIG. 4. Theoretical and experimental nonresonant spectra for C_{60} and $C_{60}Ti$ compounds.

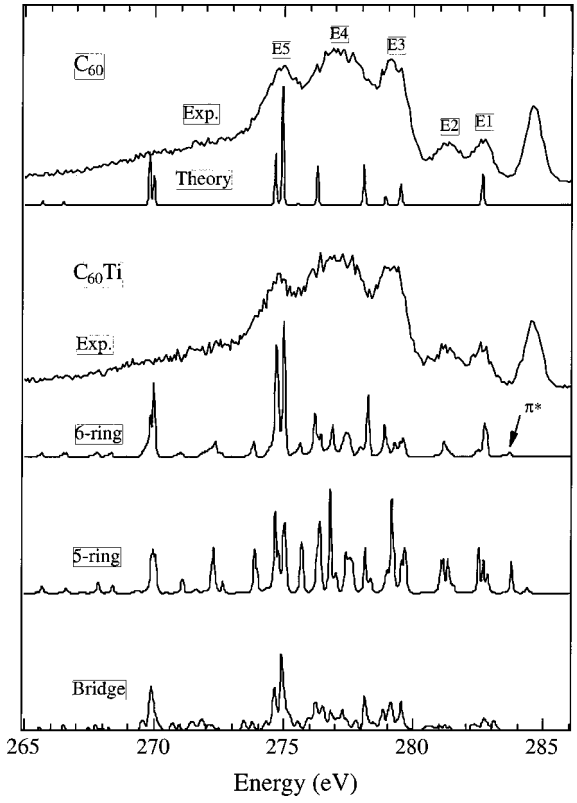

FIG. 5. Theoretical and experimental resonant spectra for C_{60} and $C_{60}Ti$ compounds.

principal difference between the two methods is the lack of dynamical correlation in Hartree-Fock, which could cause this difference.

The differences in the calculations between C_{60} and the different $C_{60}Ti$ complexes are mainly found for the outermost orbitals. Especially, for $C_{60}Ti$ η^5 and η^6, distinct peaks, labeled $\tilde{\pi}$, appear above the state corresponding to the HOMO of C_{60}, which can be interpreted as being due to the bonding. However, such extra peaks cannot be resolved in the experimental spectrum. Therefore, based on the experimental nonresonant x-ray emission spectra, it is not possible to distinguish the $C_{60}Ti$ η^6, η^5, and η^2 conformations.

B. Resonant x-ray emission

The calculated resonant x-ray emission of C_{60} for the first π^* orbital is in poor agreement with its experimental counterpart, see Fig. 5. A similar spectrum was also obtained from the previous Hartree-Fock calculations by Luo *et al.*[8] In that investigation, the discrepancies were mainly attributed to the involvement of vibronic coupling in the intermediate state of the RIXS process, removing strict RIXS selection rules, which is not considered in the theoretical treatment. The π^* of C_{60} has the symmetry of t_{1u}, which is threefold degenerate. Strong Jahn-Teller distortions due to the extremely high degeneracy are thus anticipated. Unfortunately, calculations on the effects of vibronic coupling can only be done for small molecules, like CO_2.[22,23] At present, it is not possible to explicitly treat vibronic coupling effects for C_{60} due to the size of the system. However, the effect of vibronic coupling can effectively be excluded by tuning the excitation energy as far as possible from the main resonance. Upon detuning, the RIXS spectrum can then be purified in the sense that the electronic dipole selection rules are reinforced. This has been observed experimentally for C_{60},[8] and CO_2,[22] and a general theory has also been provided.[23] The implications of the detuning spectra for $C_{60}Ti_x$ compounds will be discussed in the next section.

Considering the resonant $C_{60}Ti$ spectra for excitation into the π^* orbital, one can see an intensity increase in the region where C_{60} experimentally exhibits the symmetry-forbidden features. For instance, the E2 feature is not present in the calculated C_{60} π^* resonant spectrum due to symmetry reasons. For $C_{60}Ti$, the E2 feature is very small for the bridge adsorption site, more visible for the six-ring and very large for the five-ring adsorption site. For the five-ring adsorption site, we see that besides the E2 feature, E3 and E4 are also enhanced, which we attribute to a strong interaction of the t_{1u} orbital with the metal levels, leading to a split of the previously degenerate t_{1u} levels. The strict selection rules for RIXS that are present for C_{60} are thus, in principal, removed. Note that the bridge and the six-ring adsorption case seem to partially obey the RIXS selection rules of C_{60}, which is an indication that the interaction between the t_{1u} orbital and the metal levels is smaller for these cases. By comparing this to the nonresonant spectra in Fig. 4, we see that some of the metallic states $\tilde{\pi}$ for the six-ring adsorption case are disap-

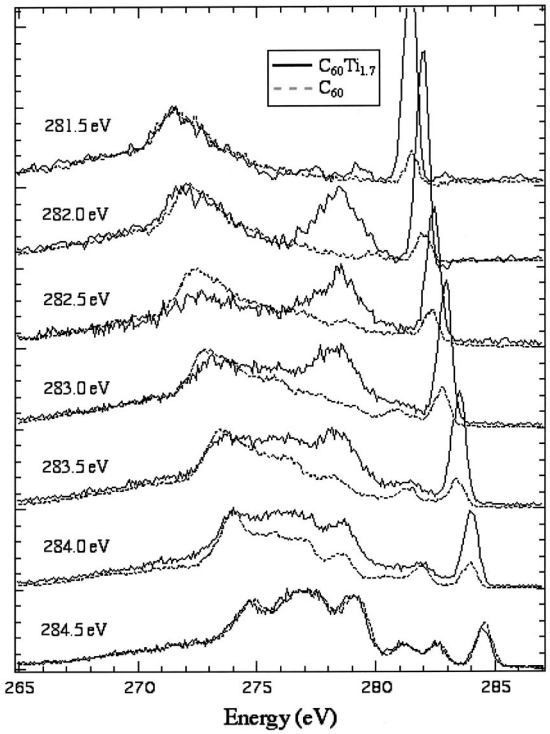

FIG. 6. Experimental detuning spectra for C_{60} and the $C_{60}Ti_{1.7}$ compound.

peared in the resonant spectrum as compared to the nonresonant case. It indicates that the symmetry of these missing states should be gerade, since gerade states are suppressed in intensity when the initial excitation is done into an ungerade state, which is the case here. These states could stem from a donation from the previously unoccupied t_{1g} orbital, or it could be due to a hybridization between the occupied $4g_g$ and $7h_g$ orbitals with the metal. In the theoretical five-ring spectrum, these states are not suppressed in the resonant spectrum, which means that in this case they are of ungerade symmetry.

Experimentally, we do not expect to be able to distinguish the different adsorption sites in the resonant spectra, since vibronic coupling is present also for $C_{60}Ti$ compounds, which makes all the spectra resemble the one of the C_{60} gas phase.

C. Detuning spectra

In the C_{60} case, we know that by detuning the excitation energy from the π^* resonance, the interaction time becomes much shorter than the lifetime of the carbon core-excited state.[22] Consequently, the vibronic coupling in the intermediate states of π^* channel (channel 1 in Fig. 3) is eliminated. For the $C_{60}Ti$ complexes, the hybridized orbitals will become resonantly excited upon detuning. Since the lifetime of the metal-carbon state is often very short, the vibronic coupling effects in the RIXS detuning process of the metal fullerene complexes will be negligible, and a better agreement between theoretical and experimental spectra is thus expected.

In Fig. 6 we display the experimental detuning spectra of C_{60} and $C_{60}Ti$, with varying incoming photon energies. As

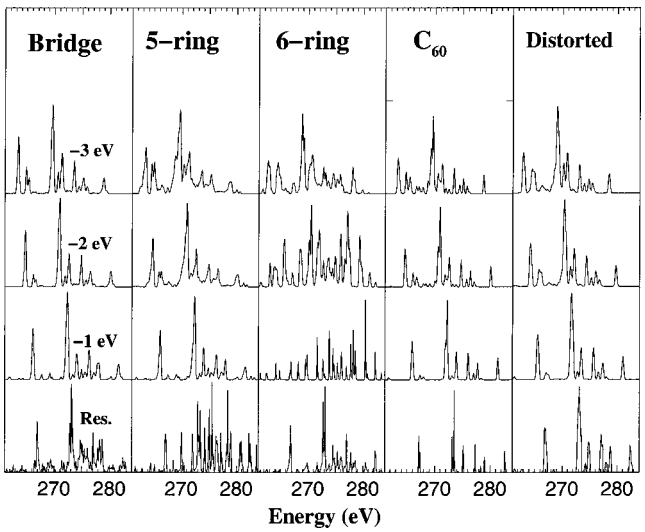

FIG. 7. Theoretical detuning spectra for the different $C_{60}Ti_1$ models, for C_{60} and for a distorted C_{60} molecule in the geometry of the $C_{60}Ti_1$ system, but without inclusion of the Ti.

expected, the C_{60} spectra exhibit typical Raman shifts, and the spectral shape changes and resembles the theoretical resonant spectrum for C_{60} at large detuning energies; the process consequently follows the strict RIXS selection rules. The $C_{60}Ti$ spectra behave in a different manner. Upon detuning, the E5 feature behaves like the one in the pure C_{60} spectra, exhibiting a Raman shift. However, a new, strong feature in the energy region between 277 and 279 eV appears and is enhanced in intensity for detuning energies between 1.0 and 2.5 eV, and shows no Raman shifting at all. The appearance of this feature indicates that there are other scattering channels with a RIXS selection rule different from the one for C_{60} that is involved at this energy region. It thus means that new hybridization states have symmetries that are different from the main π^* level.

In order to further understand this, and to see if similar effects can be observed also in calculations, we have generated theoretical RIXS detuning spectra for C_{60} and $C_{60}Ti_1$, see Fig. 7. This figure shows three series of spectra for the $C_{60}Ti_1$ corresponding to the three different adsorption sites for Ti (η^2, η^5, and η^6). Two more series of spectra are displayed for pure C_{60} and ''distorted'' C_{60}. The ''distorted'' spectra are calculated for C_{60} in the geometry of $C_{60}Ti_1$ (η^6), without inclusion of the Ti atom, which is very similar to the pure C_{60} ones except for a small overall shift, and a small increase in intensity at about 277–279 eV. It can be concluded that the geometry effect alone cannot cause the spectral shape changes that were found experimentally, but instead, the bonding to the metal atoms must be responsible for this.

The symmetry of the intermediate states has a strong impact on the appearance of the RIXS spectrum. If the metallic states consist of the t_{1u} orbital hybridized with the metal, the emission spectra from these channels will have almost the same profile as those from the π^* channels. Instead, if the metallic states consist of another C_{60} molecular orbital hybridized with the metal, e.g., the HOMO of C_{60} ($4h_u$), the RIXS selection rules will change the shape of the emission

spectrum according to the selection rules governed by the symmetry of the intermediate state.

As can be seen from Fig. 7, the bridge and the five-ring emission spectra both exhibit a Raman shift of the main intensity. This indicates that the hybridized orbitals possess a similar symmetry as the π^* orbital of C_{60}. Therefore, the bonding mainly involves the mixing of the Ti d orbitals with the π^* orbital of C_{60} (t_{1u}), a donation mechanism.

Note that the five-ring $C_{60}Ti_1$ detuning spectra behave like the experimental C_{60} ones upon detuning. The symmetry ''forbidden'' states that are present at resonance disappear, which can easily be understood in the following way; when we are resonant to the main peak (which in the five-ring case is no longer degenerate), we pick up one of the three t_{1u} components. The RIXS interference terms do not cancel any more than they did for C_{60}, since we now have an energy separation between the t_{1u} derived scattering channels. When we detune the energy, the energy separation between the t_{1u} scattering channels becomes relatively smaller in comparison with the detuning energy, and the three components of t_{1u} behave like a single-scattering channel. When this happens, the interference effects will act as if the states are degenerate again, leading to strict RIXS selection rules like we have for C_{60}.

In contrast to the bridge and five-ring adsorption cases, the six-ring x-ray emission spectra show an extra high intensity feature towards higher energies, similar to what was observed in the experiments. It thus means that the hybridized orbitals should have a different symmetry than the π^* orbital of C_{60}, since an involvement of only the t_{1u} orbital does not change the spectral shape. According to the DCD model, the symmetry of the orbitals should be close to the symmetry of the HOMO of C_{60}, (h_u). Actually, it has been shown in the previous study of RIXS for C_{60} (Ref. 8) that the resonant x-ray emission spectrum of C_{60} at an excitation energy matching with the LUMO+4 level, which has h_u symmetry, has a dominant intensity in the region 277–279 eV, close to what we have observed in the experimental and calculated detuning spectra presented in this paper. Therefore, the hybridization orbitals have a close resemblance to the h_u symmetrical ones for C_{60}. It is not straightforward to conclude this from investigations of the wave function, since the symmetry is strictly broken, but the use of RIXS spectroscopy can seemingly help us in the characterization of the hybridization states.

The interaction between Ti and C_{60} will introduce a chemical shift of the carbon core levels. The maximum core-level energy shift is found to be around 0.5 eV based on Koopman's theorem, which is in reasonably good agreement with the experimental value of 0.36 eV for $C_{60}Ti_2$.[7] This small core-level shift seems not to be responsible for the spectral shape changes that are found here, but the spectral shape changes, as we mentioned before, stem from new hybridization levels.

In addition to the donation of charge from h_u to the metal, we expect to have also a large donation from the metal to the LUMO of C_{60}. In fact, our calculations give Mulliken charges of +0.8 of the metal for the six-ring and five-ring cases, and +0.4 for the bridge case, which correspond to substantial charge donations from the metal. The Ti atom is in the six-ring case close to a $3d^3 4s^0$ configuration as compared to the atomic $3d^2 4s^2$ configuration, which indicates that all of the $4s$ electrons have been removed, probably in order to minimize the Pauli repulsion towards the fullerene. The charge of the carbon atoms directly involved in the bond is, on an average, 0.05 excess electrons per carbon atom, which shows that the charge donated from the metal is quite delocalized on the fullerene.

Note that this large donation of charge from the metal should be possible to detect in the different x-ray emission spectroscopy (XES) spectra. Very little evidence is found for this in the experimental spectra, though, but in the nonresonant XES spectra, Fig. 4, we see a small tail in the region between 283–285 eV. These states are easily seen for $C_{60}Ti_{3.6}$, (see Ref. 7), which we interpret as the charge donated from the metal.

In our calculations, we have a few discrete hybridization states due to the small cluster model, but for the compound we expect more of a band formation for the metallic levels. We base this on the fact that the feature between 277–279 eV in the detuning spectra does not Raman shift when we change the photon energy. This indicates that there is a band of hybridization states formed so that we are always exciting resonantly into these states, which in turn show no Raman shift.

To summarize this section, we conclude that in addition to the donation mechanism from the metal into the t_{1u} orbital of C_{60}, we now also seem to have experimental indications of a back donation from the HOMO of C_{60} to the metal, based on the detuning spectra.

VI. CONCLUSIONS

In this paper, we have introduced RIXS spectroscopy as a means for understanding chemical bond formation between a metal (Ti) and C_{60}. We have used simple $C_{60}Ti$ cluster models within the DFT framework, in order to interpret experimental RIXS spectra of $C_{60}Ti$ compounds. A comparison between experiment and theory leads us to propose a bonding mechanism that involves both the HOMO $(4h_u)$ and the LUMO (t_{1u}) interacting with the metal. We further suggest, in line with other previous investigations, that Ti prefers a six-ring bonding site on the fullerene, based on the RIXS data and on total-energy calculations. It is our belief that RIXS detuning spectroscopy can be used not only for understanding the bond formation in this system, but also for many other organometallic compounds, where the bonding breaks the symmetry of the ligand of the metal.

[1] A. F. Hebard, M. J. Rosseinski, R. C. Haddon, D. W. Murphy, S. H. Glarum, T. Palstra, A. P. Ramirez, and A. R. Kortan, Nature (London) **350**, 600 (1991).
[2] A. L. Balch and M. M. Olmstead, Chem. Rev. **98**, 2123 (1998).
[3] I. Amos B. Smith, *Fullerene Chemistry* (Pergamon, Oxford, 1996).
[4] W. Andreoni, Annu. Rev. Phys. Chem. **49**, 405 (1998).
[5] S. Nagao, T. Kurikawa, K. Miyajima, A. Nakajima, and K. Kaya, J. Phys. Chem. A **102**, 4495 (1998).
[6] L. Norin, U. Jansson, C. Dyer, P. Jacobsson, and S. McGinnis, Chem. Mater. **10**, 1184 (1998).
[7] L. Qian, L. Norin, J.-H. Guo, C. Såthe, A. Agui, U. Jansson, and J. Nordgren, Phys. Rev. B **59**, 12 667 (1999).
[8] Y. Luo, H. Ågren, F. Gel'mukhanov, J. Guo, P. Skytt, N. Wassdahl, and J. Nordgren, Phys. Rev. B **52**, 14 478 (1995).
[9] J. P. Perdew and Y. Wang, Phys. Rev. B **45**, 13 244 (1992); J. P. Perdew, in *Electronic Structure of Solids*, edited by P. Ziesche and H. Eischrig (Akademie Verlag, Berlin, 1991); J. P. Perdew, J. A. Chevary, S. H. Vosko, K. A. Jackson, M. R. Pederson, D. J. Singh, and C. Fiolhais, Phys. Rev. B **46**, 6671 (1992).
[10] DEMON-KS version 4.0, M. E. Casida, C. Daul, A. Goursot, A. Koester, L. G. M. Pettersson, E. Proynov, A. St-Amant, D. R. Salahub, principal authors, H. Duarte, N. Godbout, J. Guan, C. Jamorski, M. Leboeuf, V. Malkin, O. Malkina, M. Nyberg, L. Pedocchi, F. Sim, L. Triguero, and A. Vela, contributing authors, DEMON Software, 1997.
[11] Y. Luo, H. Ågren, and F. Gel'mukhanov, J. Phys. B **27**, 4169 (1994).
[12] Y. Luo, H. Ågren, J. Guo, P. Skytt, N. Wassdahl, and J. Nordgren, Phys. Rev. A **52**, 3730 (1995).
[13] J. H. Guo, M. Magnuson, C. Såthe, J. Nordgren, L. Yang, Y. Luo, H. Ågren, K. Xing, N. Johansson, and W. Salaneck, J. Chem. Phys. **108**, 5990 (1998).
[14] L. Triguero, Y. Luo, L. G. M. Pettersson, H. Ågren, P. Väterlein, M. Weinelt, A. Fölish, J. Hasselström, O. Karis, and A. Nilsson, Phys. Rev. B **59**, 5189 (1999).
[15] T. Warwick, P. Heimann, D. Mossessian, W. McKinney, and H. Padmore, Rev. Sci. Instrum. **66**, 2037 (1995).
[16] J. Nordgren, G. Bray, S. Cramm, R. Nyholm, J. E. Rubensson, and N. Wassdahl, Rev. Sci. Instrum. **60**, 1690 (1989).
[17] A. Nakajima, S. Nagao, H. Takeda, T. Kurikawa, and K. Kaya, J. Chem. Phys. **107**, 6491 (1997).
[18] T. Kurikawa, S. Nagao, K. Miyajima, and K. Kaya, J. Phys. Chem. **102**, 1743 (1998).
[19] A. N. Andriotis and M. Menon, Phys. Rev. B **60**, 4521 (1999).
[20] M. Dewar, Bull. Soc. Chim. Fr. **18**, C79 (1951).
[21] J. Chatt and L. Duncanson, J. Chem. Soc. 2939 (1953).
[22] P. Skytt, P. Glans, J. H. Guo, K. Ginnelin, C. Såthe, J. Nordgren, F. K. Gel'mukhanov, A. Cesar, and H. Ågren, Phys. Rev. Lett. **77**, 5035 (1996).
[23] A. Cesar, F. Gel'mukhanov, Y. Luo, H. Ågren, P. Skytt, P. Glans, J.-H. Guo, K. Gunnelin, and J. Nordgren, J. Chem. Phys. **106**, 1827 (1997).